



Article

# Synthesis, Computational Studies and Characterization of Some a Novel Charge-transfer Complexes Derivative from 4-(11-methyltriphenylen-2-Yl)-1,2,3-selenadiazole

Haider Shanshool Mohammed<sup>\*1</sup>

1. Department of Environmental Health, College of Applied Medical Sciences, University of Al-Muthanna, Muthanna, Iraq

\* Correspondence: [haider.shanshool@mu.edu.iq](mailto:haider.shanshool@mu.edu.iq)

**Abstract:** A new group of charge-transfer complexes, of chemical material were synthesized in the current study using a direct method with a good yield. We reacted 4-(11-methyltriphenylen-2-yl)-1,2,3-selenadiazole with four different types of quinones in a 1:1 mole ratio, using acetonitrile as the solvent. Each compound was identified with the help of analytical techniques like mass spectroscopy, <sup>1</sup>H-NMR, UV, and IR. The chemical structures suggested for the synthesized compounds were in agreement with the analysis findings. The DFT (functional theory of density) was utilized to analyze, the structure of the molecules of the developed charge-transfer complexes. During the process of geometry optimization, the HOMO, LUMO surfaces, and energy gap were created utilizing the (3-21G) as the base set of geometrical structures. Charge-transfer, complex-containing compounds' molecular outlines and geometry have been evaluated through the geometrical optimization process. Through the study of donor-acceptor interactions, we have also been comparing the HOMO energies of the molecules in charge-transfer complexes. On the other hand, it was calculated and analyzed the gap energy, ionization potential, electron affinity, electronegativity, and electrophilicity of compounds containing charge-transfer complexes.

**Keywords:** DFT, Charge-transfer Complexes, Geometry Optimization, Electron Affinity, 4-(11-Methyltriphenylen-2-Yl)-1,2,3-selenadiazole

**Citation:** Mohammed, H. S. Synthesis, Computational Studies and Characterization of Some a Novel Charge-transfer Complexes Derivative from 4-(11-methyltriphenylen-2-Yl)-1,2,3-selenadiazole. Central Asian Journal of Theoretical and Applied Science, 6(2), 135-154.

Received: 1<sup>st</sup> Feb 2025

Revised: 2<sup>nd</sup> Feb 2025

Accepted: 10<sup>th</sup> Feb 2025

Published: 20<sup>th</sup> Feb 2025



**Copyright:** © 2025 by the authors. Submitted for open access publication under the terms and conditions of the Creative Commons Attribution (CC BY) license (<https://creativecommons.org/licenses/by/4.0/>)

## 1. Introduction

The organic charge-transfer complexes consist of two systems consisting of two electrons, with a specific stoichiometry; a donor, and an acceptor electron unit. A lot of research has been done on charge-transfer complexes for a long time in an attempt to provide guidelines for the manufacturing of substances possessing strong superconductivity or mobility at room temperature [1]. However, the creation of increasingly complex technological applications using these charge-transfer complexes [2-3] has drawn attention recently as well. The following are some examples: organic field-effect transistors (OFTs) [4-5], thermoelectric [6-7], photoconductors [8-9], strain sensors [10], and ferroelectrics, when CT compound complexes are utilized as either organometals [11-12] or organo semiconductors, [13-14]. It has long been established that organoselenium compounds are very pertinent molecules. Practically speaking, aside from being helpful intermediary compounds in organic compound synthesis, for examining fundamental issues in Chemistry of theory [15-18], Compounds of Organoselenium have special characteristics that make them perfect for synthesis; atoms of selenium can be

removed by appropriate procedures for instance, oxidation, which creates a double bond, via means of synelimination with selenium oxide [19]. and selenium-containing fragments are easily integrated into organic molecules. The interaction between selenious acid and semicarbazone is widely recognized to provide the basis for the Almost all of the procedures used, to produce selenadiazole organo compounds, [20–22]. In this work, four distinct types of quinones, such as 1,2-benzoquinone, 1,4-anthraquinone, 9-hydroxy-1,4-anthraquinone, and 7,7,8,8-tetracyanoquinodimethane, will be reacted to produce new charge-transfer complexes. using 4-(11-methyltriphenylen-2-yl)-1,2,3-selenadiazole to synthesize new molecules with the ability to transfer charges.

## 2. Materials and Methods

### Materials

The substances that were used were 1,2-benzoquinone (Sigma-Aldrich), 1,4-anthraquinone (Fluka), 7,7,8,8-tetracyanoquinodimethane (Strem Chemicals), ethanol absolute and acetonitrile (Sigma-Aldrich Inc.), 1-(8-methyltriphenylen-2-yl)ethan-1-one and hydrazinecarboxamide (Fluka), and 9-hydroxy-1,4-anthraquinone (Fluka).

**The computational study Program:** Computational study program: Gaussian 09W set with approximated DFT-based descriptors and a basis of 3–21G.

### Instrumental

UV-visible spectrophotometer model number UV-1650 (Japan) (Shimadzu Double-beam) with (1.00 cm) of quartz cell, and an apparatus with a melting point that is electrothermal. spectra of  $^1\text{H-NMR}$  were acquired using 500 MHz spectrometers made by Bruker that use TMS as an internal reference and soluble DMSO- $d_6$ . Spectra infrared FT-IR With a Shimadzu model 8400 S spectrophotometer, the wave number range for KBr is 4000-400  $\text{cm}^{-1}$ .

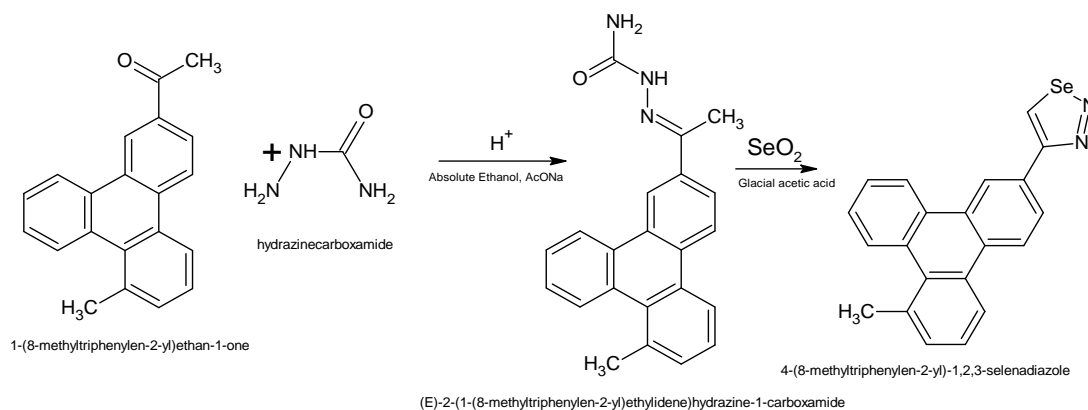
### Procedure

#### 1. Preparation compound (E)-2-(1-(8-methyltriphenylen-2-yl)ethylidene)hydrazine-1-carboxamide. [23]

A mixture of 2.58 g (9.1 mmol) of 1-(8-methyltriphenylen-2-yl)ethan-1-one, 1.5 g (20.0 mmol) of hydrazinecarboxamide, 1.78 g (21.8 mmol) of sodium acetate, and 11 mL of absolute ethanol was refluxed for 48 hours at 80°C while stirring. by diluting the reaction mixture with 30 mL of water, filtering off the pink-colored crystal precipitate, and letting it dry in the air. A 69% yield and a melting point of 133–135 °C were obtained. TLC detected the end of the reaction with an  $R_f$  value of 0.82 (3:7) (n-hexane: ethyl acetate). like in Scheme 1.

#### 2. Preparation compound 4-(11-methyltriphenylen-2-yl)-1,2,3-selenadiazole) MTSD [24]

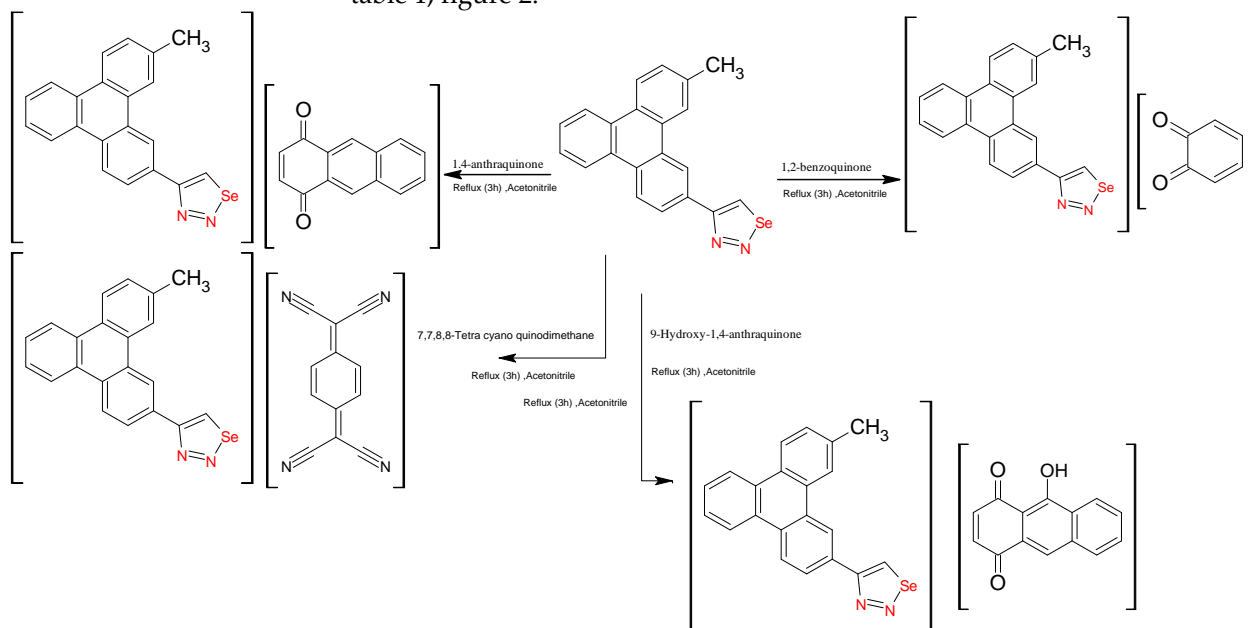
A mixture of 2.3 g (6.75 mmol) of (E)-2-(1-(8-methyltriphenylen-2-yl)ethylidene)hydrazine-1 carboxamide, 0.9 g (8.1 mmol) of selenium dioxide, and 13.5 mL of glacial acetic acid was stirred for 20 h at 60°C. The crystals that formed were then filtered off after the reaction mixture had been diluted with 40 milliliters of water. The resulting precipitate was dissolved in acetone, allowed to coagulate the colloid selenium for one hour, and filtration was done on the mixture. After removing the acetone, boiling hexane was used to extract the residue. coffee Crystals were created as the hexane evaporated. A 68% yield and a melting point of 113–115 °C were obtained. TLC detected the end of the reaction with an  $R_f$  value of 0.86 (3:7) (n-hexane: ethyl acetate). like in figure 1.



**Figure 1.** Preparation of 4-(11-methyltriphenyl-2-yl)-1,2,3-selenadiazole (MTSD).

### Preparation charge transfer complexes (MTSDQ1, MTSDQ2, MTSDQ3, MTSDQ4).

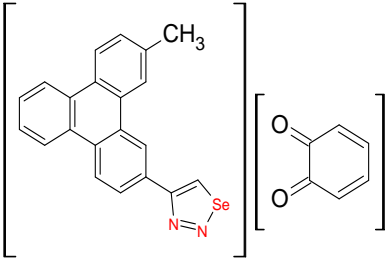
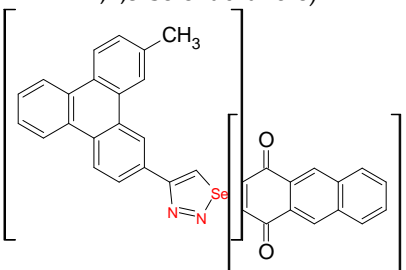
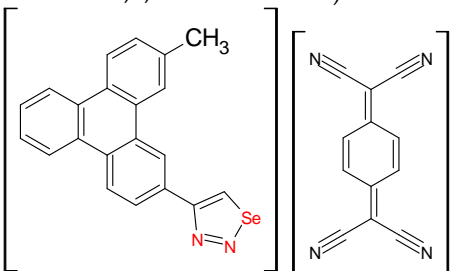
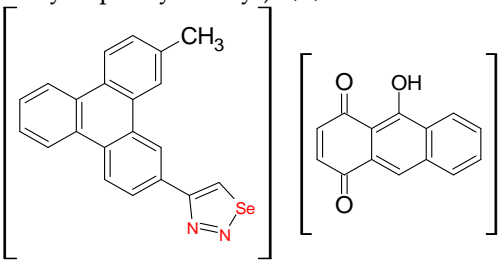
The compound MTSD (1.492 g, 4 mmol) was dissolved in 60 mL of acetonitrile and combined with four different types of quinones, each separately (1,2-benzoquinone, 1,4-anthraquinone, 7,7,8,8-tetracyanoquinodimethane, and 9-hydroxy-1,4-anthraquinone). The mixture was then in a water bath, it refluxed at 100 °C for three hours. To get a variety of precipitate colors and yields, the solution was chilled, evaporated, using a rotating evaporator, as well as then rinsed with a tiny amount of acetonitrile, [23, 24]. A melting point was then measured. TLC observed the conclusion of the reaction, as indicated in table 1, figure 2.



**Figure 2.** Synthesis steps for charge transfer complexes (MTSDQ1, MTSDQ2, MTSDQ3, and MTSDQ4).

**Table 1.** The physical characteristics and chemical properties for synthesis complexes of charge- transfer (MTSDQ1, MTSDQ2, MTSDQ3, and MTSDQ4).

structure and physical properties of synthesized compounds							
seq	Quinone	Weight of Quinone	Structure of synthesized compounds and symbol	yield of compound	melting point	Rf value	Appearance

1.	1,2- benzoquin one	1.925 g	 <p>MTSDQ1 (1,2-benzoquinone-4-(11-methyltriphenylen-2-yl)- 1,2,3-selenadiazole)</p>	72%	103-104 °C	0.74	Light - yellow
2.	1,4- anthraquin one	2.32 g	 <p>MTSDQ2 (1,4-Anthraquin- 4-(11-methyltriphenylen-2-yl)- 1,2,3-selenadiazole)</p>	89%	107-109 °C	0.68	Dark - yellow
3.	7,7,8,8- Tetracyano quinodimet hane	2.31 g	 <p>MTSDQ3 (7,7,8,8-Tetracyanoquinodimethane-4-(11- methyltriphenylen-2-yl)-1,2,3-selenadiazole)</p>	85%	141 - 142°C	0.73	brown
4.	9-Hydroxy- 1,4- anthraquin one	2.39 g	 <p>MTSDQ4 (9-Hydroxy-1,4-anthraquino-4-(11- methyltriphenylen-2-yl)-1,2,3-selenadiazole)</p>	79%	155-157 °C	0.91	Light- red

### 3. Results and Discussion

In this work, 4-(11-methyltriphenylen-2-yl)-1,2,3-selenadiazole (MTSD) was reacted to create charge transfer complexes (prepared in the third step) [23, 24]. Four distinct quinones, each with a unique reaction, were then added in acetonitrile as a solvent to produce new compounds (MTSDQ1, MTSDQ2, MTSDQ3, MTSDQ4). The novel charge transfer complexes' UV-visible spectra that were obtained from compounds MTSD with quinones included the  $n-\pi^*$  transitions, which usually undergo a notable blue shift during the synthesis of complexes of charge transfer. The diverging electron cloud surrounding the selenium atom and the shift in the charge-transfer complexes' development are caused by the selenium atom. The transition values ( $\pi-\pi^*$ , and  $n-\pi^*$ ) decrease when the electron donors of quinones decrease.

[25], the absorption bands shifted to shorter wavelengths, and the conjugate effects of the chromophore group raised the energy needed for the  $\pi$ - $\pi^*$  and  $n$ - $\pi^*$  transitions [26]. Table 2 presents these, and Figures 1-4 show them.

**Table 2.** Charge transfer complexes of specific compounds with  $\lambda$  max of ( $\pi$ - $\pi^*$ , and  $n$ - $\pi^*$ ) transitions.

Seq.	Compound.	$\lambda$ max of ( $\pi$ - $\pi^*$ , and $n$ - $\pi^*$ ) transitions
1	MTSDQ1	(218, 240, 255, 275, 340) nm
2	MTSDQ2	(206, 228, 257, 273, 347) nm
3	MTSDQ3	(207, 218, 254, 280, 405) nm
4	MTSDQ4	(202, 241, 288, 327, 483, 581) nm

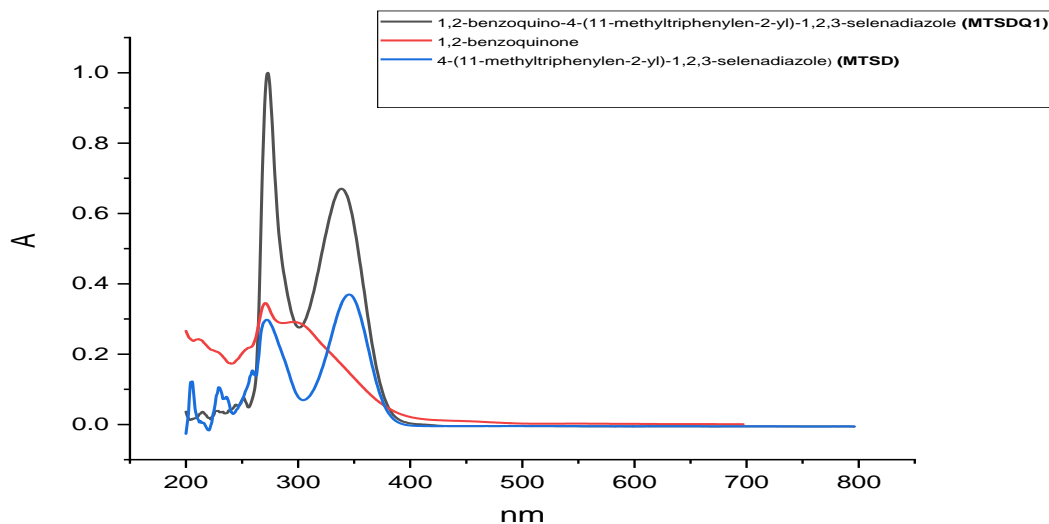


**Figure 3.** UV-Visible spectrum of charge-transfer complex compound (MTSDQ1).

In the compound's spectra, the charge-transfer absorption band (MTSDQ1) appears between 255 and 300 nm.

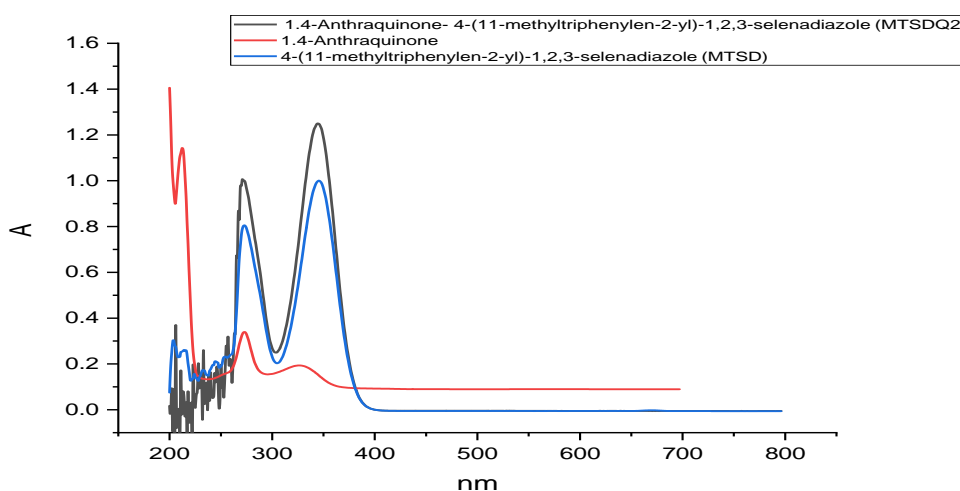


**Figure 3.** UV-Visible spectrum of charge-transfer complex compound (MTSDQ2).

In the compound's spectra, the charge-transfer absorption band (MTSDQ2) appears between 310 and 390 nm.

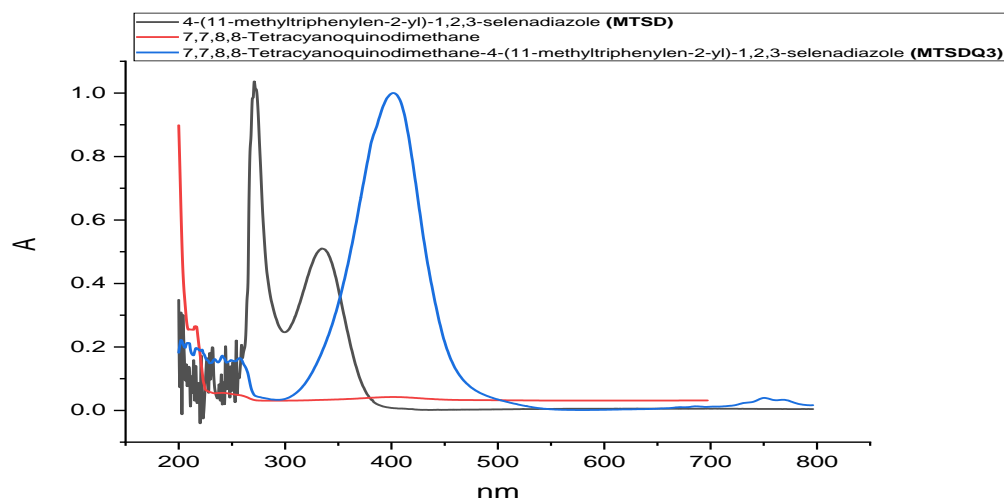


**Figure 4.** UV-Visible spectrum of charge-transfer complex compound (MTSDQ3).

In the compound's spectra, the charge-transfer absorption band (MTSDQ3) appears between 310 and 480 nm.

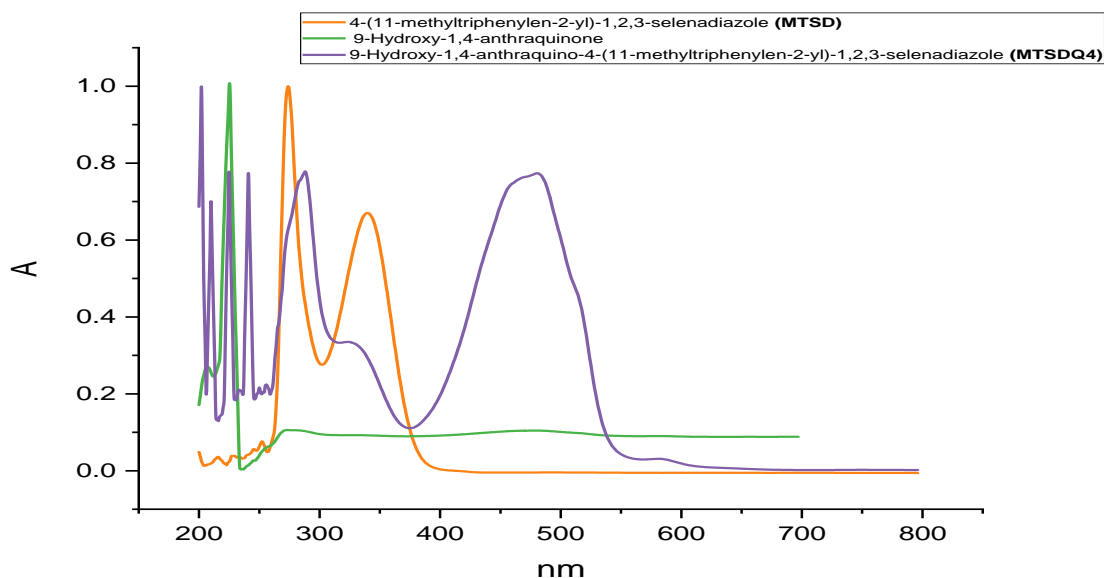


**Figure 5.** UV-Visible spectrum of charge-transfer complex compound (MTSDQ4).

In the compound's spectra, the charge-transfer absorption band (MTSDQ4) appears between 380 and 540 nm.

**Table 3.** The FT-IR beams of synthesized charge-transfer complex compounds.

Compounds	Functional group								
	C-H Ar.	C=O Ar.	C-H Aliph.	C=N Ar	C=C Ar.	C=C Aliph	C≡N Aliph	OH Ar.	C-N Ar.
MTSD	3064	-	2947	1587	1471	-	-	-	1330
MTSDQ1	3039	1639.5	2945	1573	1450	-	-	-	1325
MTSDQ2	3059	1658	2920	1577	1504	-	-	-	1325
MTSDQ3	3025	-	2970	1639.5	1543.1	1433	2225	-	1325
MTSDQ4	3020	1631	2958	1589.4	1529.6	-	-	3420	1259

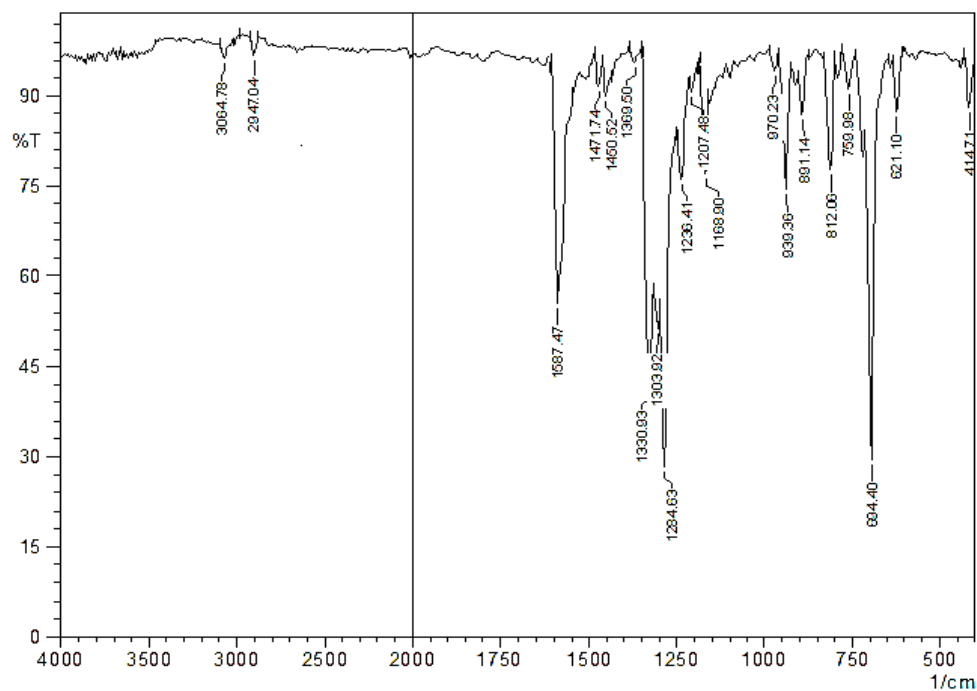


Figure 6. FT-IR spectra of compound (MTSD).

There is no carbonyl group in the compound's (MTSD) FTIR spectra.

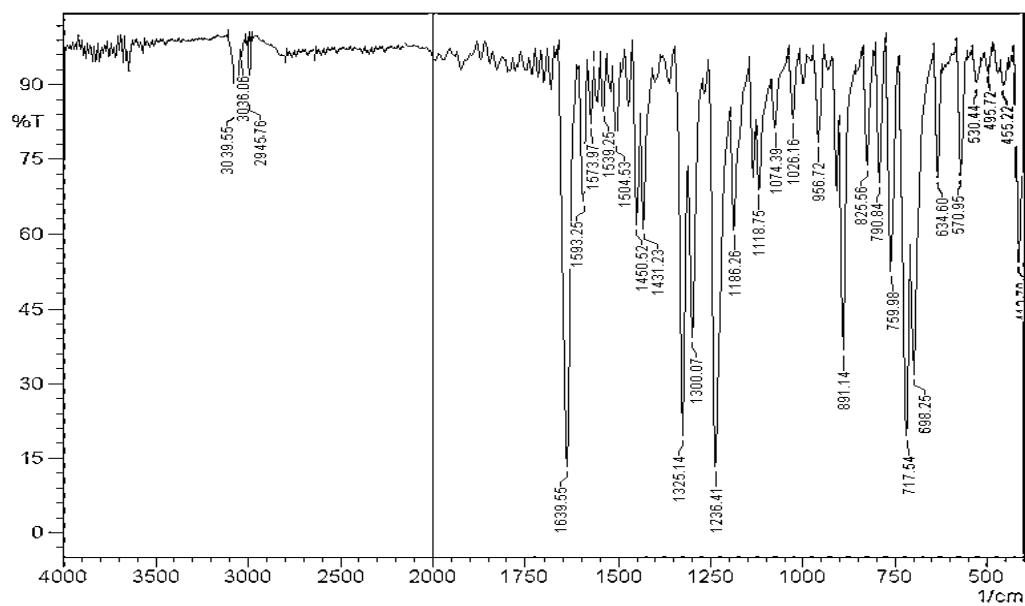


Figure 7. FT-IR spectra of compound (MTSDQ1).

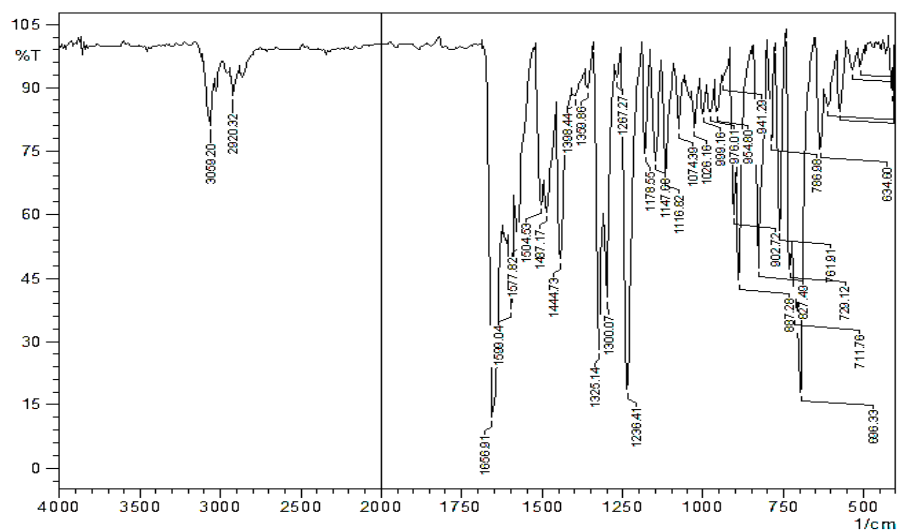


Figure 8. FT-IR spectra of compound (MTSDQ2).

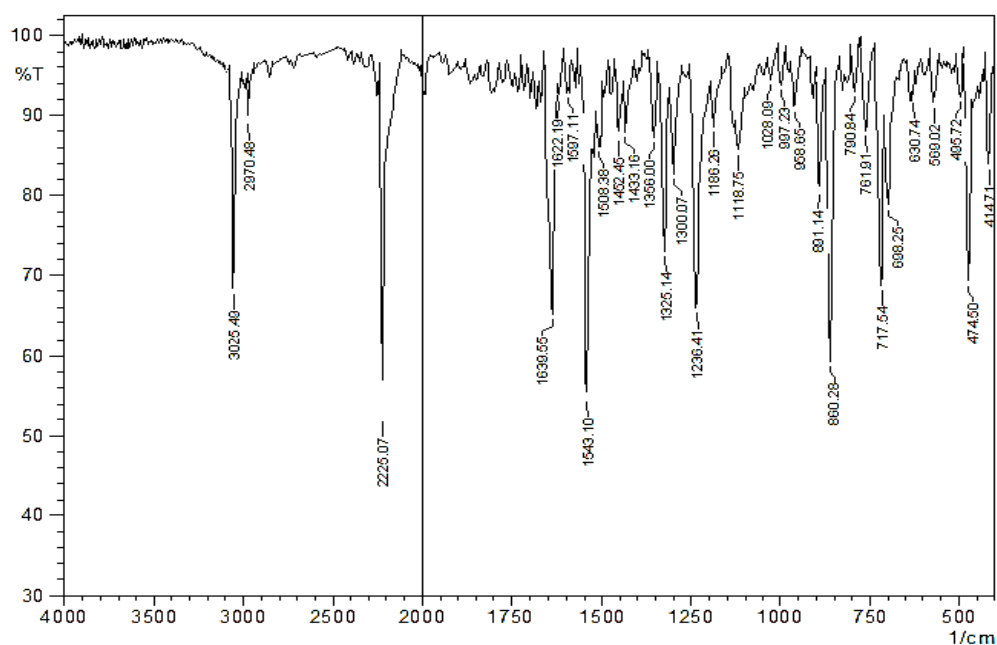
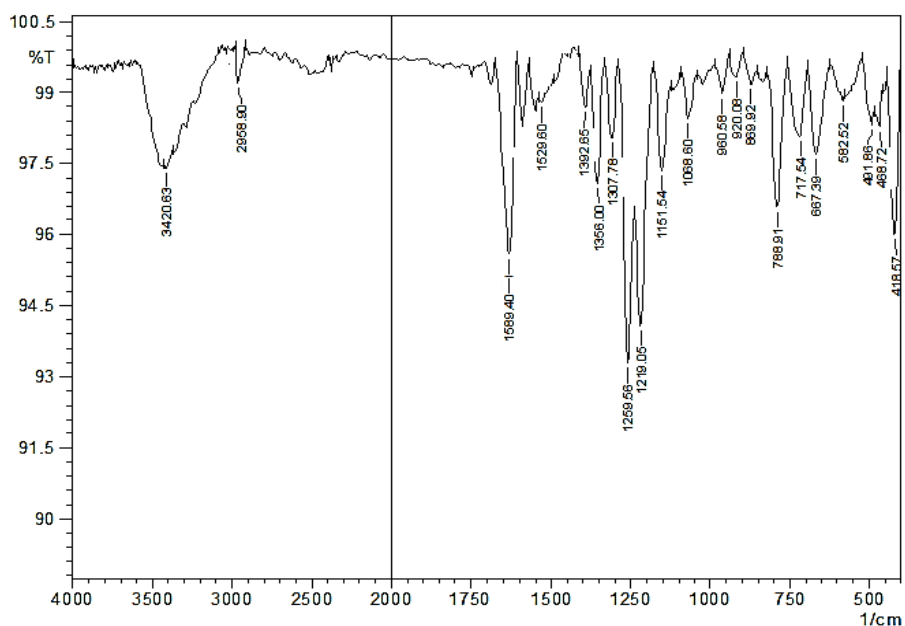


Figure 9. FT-IR spectra of compound (MTSDQ3).

The compound's (MTSDQ4) FT-IR spectra differs from other compounds' because it has a  $C\equiv N$  group and appears at  $2225\text{ cm}^{-1}$ . [27, 28]



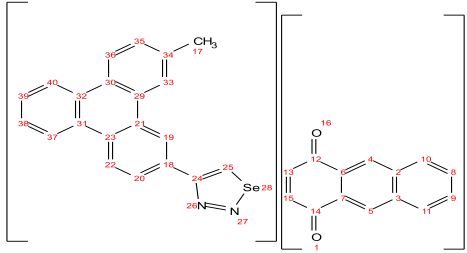
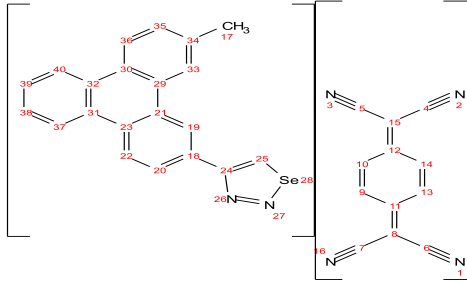
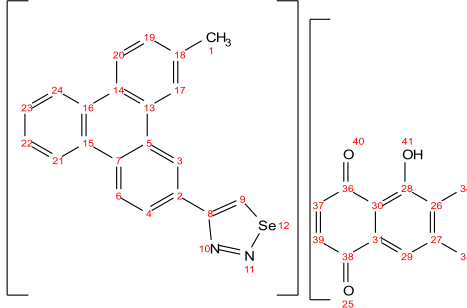
**Figure 10.** FT-IR spectra of compound (MTSDQ4).

Because the chemical (MTSDQ4) has an OH group and appears at  $3420\text{ cm}^{-1}$ , its FT-IR spectrum differs from other compounds'.

$^1\text{H-NMR}$  or (nuclear magnetic resonance spectroscopy), which finds the protons inside the chemical molecule, is one of the most crucial techniques for examining the suggested structures.  $^1\text{H-NMR}$  spectra of synthesized compounds [29] are displayed in table 4 and figures 10–14.

**Table 4.**  $^1\text{H-NMR}$  spectral data of syntheses compounds.

Seq	Compound s	Structure of the compound	$^1\text{H-NMR}$ , (DMSO- $d_6$ ); TMS = 0 ppm
1	MTSD		Alpha. 1CH <sub>3</sub> , (3H, s, 3.38); Ar. 17C-H(1H, s, 7.62); ; Ar. 19C-H (1H, d, 7.64); 20C-H (1H, d, 7.87); Ar.3C-H (1H, s, 7.88); Ar. 4C-H (1H, d, 7.89); Ar.6C-H (1H, d, 8.00); Ar.21C-H, 22C-H 23C-H, 24C-H (4H, ddt, 8.09); Ar. 9C-H (1H, s, 8.10); Ar.
2	MTSDQ1		Alpha. 9CH <sub>3</sub> , (3H, s, 3.35) ; Ar. 3C-H,4C-H (2H, tt, 7.62); Ar. 5C-H,6C-H (2H, dd, 7.71); 17C-H (1H, s, 7.74); Ar.12C-H, 14C-H (2H, d, 7.86); Ar. 30C-H 31C-H (2H,tt, 7.90); Ar.29C-H, 32C-H (2H, dd, 8.00); 27C-H, 28C-H (2H, dd, 8.02) Ar. 25C-H (1H, s, 8.10)

3	MTSDQ2		<p>Alpha. 17CH<sub>3</sub>, (3H, s, 3.40) ; Ar. 3C-H,5C-H (2H, s, 7.63); Ar. 10C-H,11C-H (2H, dd, 7.72); 25C-H (1H, s, 7.73); Ar.8C-H, 9C-H (2H, tt, 7.85); Ar. 13C-H 15C-H (2H,dd, 7.88); Ar.20C-H, 22C-H (2H, dd, 7.93); 35C-H, 36C-H (2H, dd, 7.95) Ar. 19C-H (1H, s, 7.96) Ar.38C-H, 39C-H (2H, tt, 7.99); Ar. 37C-H 40C-H (2H,dd, 8.02); Ar. 33C-H (1H, s, 8.09)</p>
5	MTSDQ3		<p>Alpha. 17CH<sub>3</sub>, (3H, s, 3.40) ; Ar. 9C-H,10C-H (2H, d, 7.63); Ar. 13C-H,14C-H (2H, dd, 7.72); 25C-H (1H, s, 7.73); Ar.20C-H, 22C-H (2H, dd, 7.93); 35C-H, 36C-H (2H, dd, 7.95) Ar. 19C-H (1H, s, 7.96) Ar.38C-H, 39C-H (2H, tt, 7.99); Ar. 37C-H 40C-H (2H,dd, 8.02); Ar. 33C-H (1H, s, 8.09)</p>
6	MTSDQ4		<p>Alpha. 1CH<sub>3</sub>, (3H, s, 3.33); Ar. 17C-H(1H, s, 7.43), ; Ar. 19C-H (1H, d, 7.96); 20C-H (1H, d, 7.97); Ar.3C-H (1H, s, 7.98); Ar. 4C-H (1H, d, 7.99); Ar. 6C-H (1H, d, 8.00); Ar.21C-H, 22C-H 23C-H, 24C-H (4H, dddd, 8.02); Ar. 9C-H (1H, s, 8.10); Ar. Ar.32C-H, 33C-H,34C-H,35C-H (4H, tddd, 8.24) Ar. 37C-H, 39C-H (2H, dd, 8.25); Ar. 29C-H (1H, d, 8.27) ; 41O-H (1H, s, 12.69)</p>

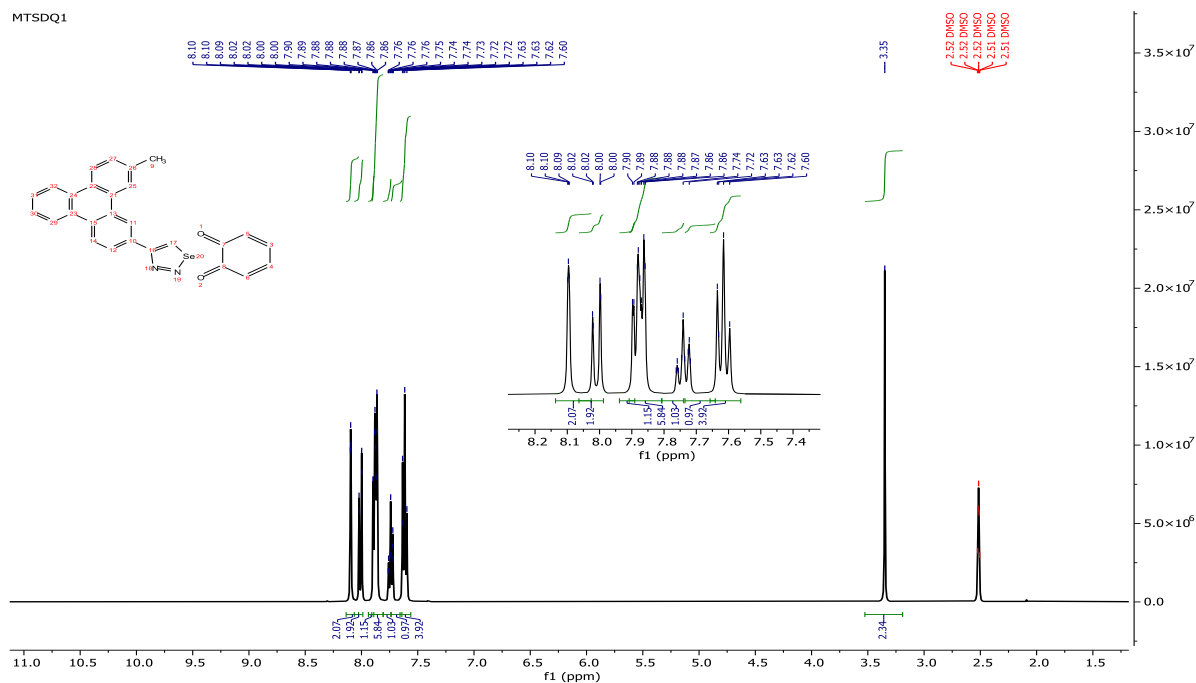


Figure 11. <sup>1</sup>H-NMR spectra of compound (MTSDQ1).



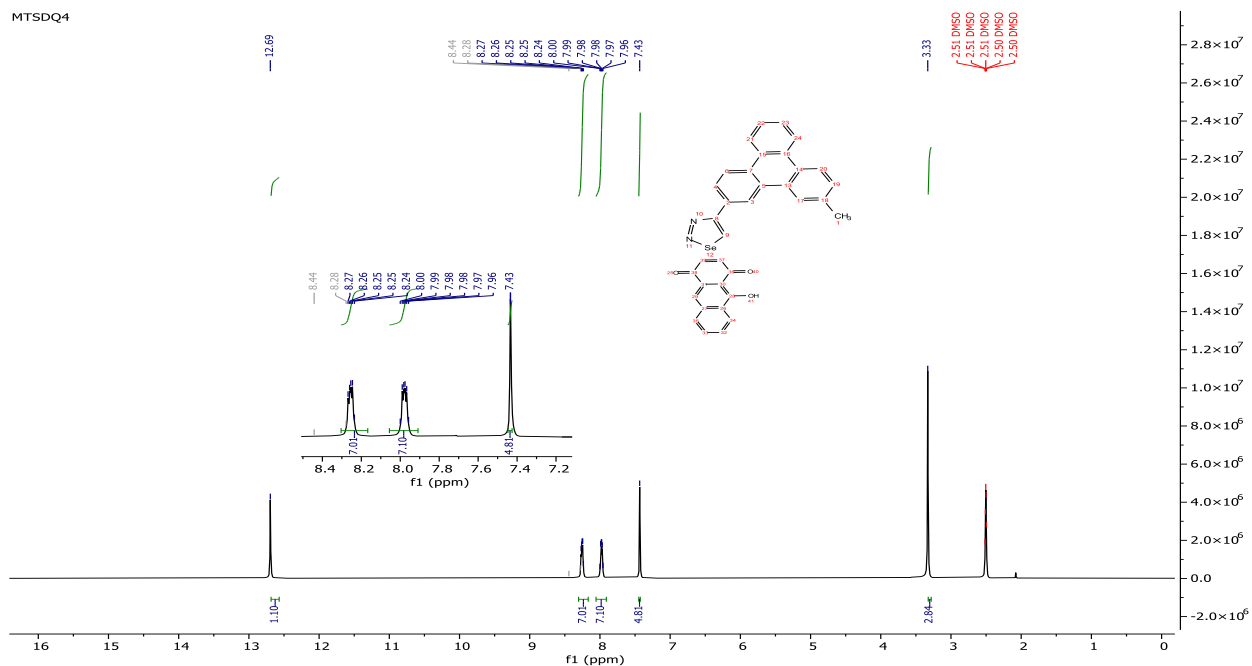
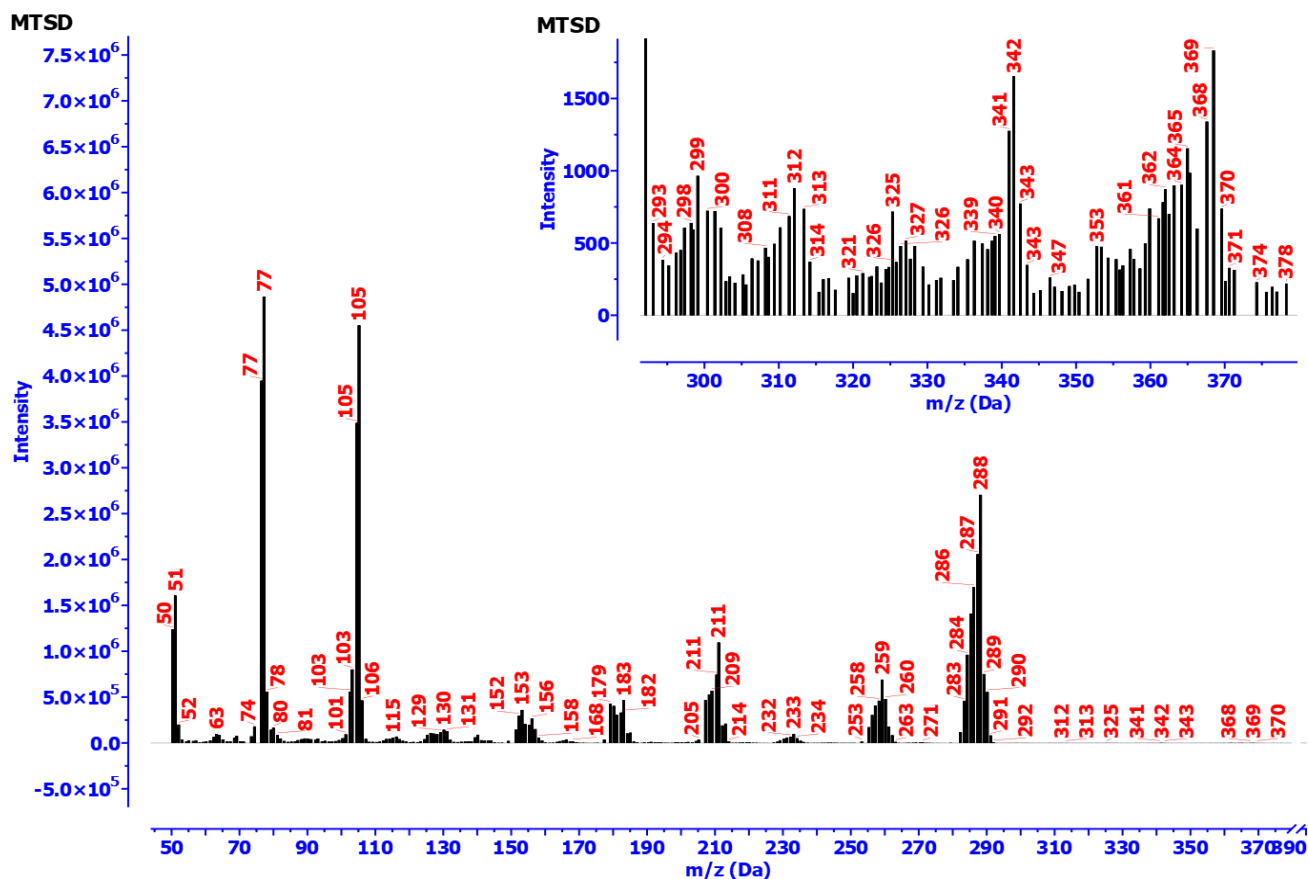


Figure 14.  $^1\text{H-NMR}$  spectra of compound (MTSDQ4).

The mass spectra signals of compound (MTSD)[30] showed us the molecular ion's parent ion beam at 376.31  $m/z$  in addition to other packages, as shown in Table 5, Figure 18, and Scheme 3.

Table 5. lists the significant peaks of compound (MTSD).

Chemical Formula:	$m/z$	Chemical Formula:	$m/z$
$\text{C}_{21}\text{H}_{14}\text{N}_2\text{Se}$	373.32	$\text{C}_{13}\text{H}_{102}\bullet$	166.08
$\text{C}_{20}\text{H}_{11}\text{N}_2\text{Se}$	359.01	$\text{C}_7\text{H}_6\bullet$	90.05
$\text{C}_{21}\text{H}_{14}\text{Se}_2\bullet$	347.03	$\text{C}_6\text{H}_4\bullet$	76.03
$\text{C}_{20}\text{H}_{11}\text{Se}_2\bullet$	331.00	$\text{CHSe}_3\bullet$	92.92
$\text{C}_{20}\text{H}_{13}\text{N}_2\bullet$	281.11	Se	77
$\text{C}_{20}\text{H}_{11}\bullet$	251.09	$\text{C}_4\text{H}_2\bullet$	50.02
$\text{C}_{19}\text{H}_{13}\bullet$	241.10		
$\text{C}_8\text{H}_4\text{N}_2\text{Se}_2\bullet$	207.95		



**Figure 15.** Mass spectrum of 4-(11-methyltriphenyl-2-yl)-1,2,3-selenadiazole (MTSD).

### Computational analysis of novel charge-transfer complex synthesizes.

The accuracy of the method in characterizing the chemical's gas phase properties was evaluated and labeled, as shown in Figs. 16 and 17. The electronic properties and these compounds' geometric structures were examined through all quantum computations at the functional computational analysis's hybrid functional (B3LYP) levels analysis utilizing the functional theory of density (DFT), which combines exchange Becke's with Parr's and Lee-Yang correlation [31–32]. In this method, each atom was described using the Gaussian (G09W) software and the set of 3–21G [36]. The mathematical correlations identified in Eqs. 1, 2, 3, and 4 as well as predicted (DFT) based descriptors were used to assess the stability and reactivity of the compounds [33–34].

$$\begin{aligned} \mu &= \left( \frac{\delta E}{\delta N} \right)_{V(\vec{r}), T} \dots\dots\dots 1 \\ \eta &= \frac{1}{2} \left( \frac{\delta^2 E}{\delta N^2} \right)_{V(\vec{r}), T} \dots\dots\dots 2 \\ S &= \frac{1}{2\eta} \dots\dots\dots 3 \\ \omega &= \frac{\mu^2}{2\eta} \dots\dots\dots 4 \end{aligned}$$

The variables  $\mu$ ,  $\eta$ ,  $S$ , and  $\omega$  stand for chemical potential, chemical hardness, chemical softness, and electrophilicity, respectively.  $E$ ,  $N$ , and  $V(\vec{r})$  represent total electron energy, electron number, and external potential, respectively. To calculate the previously indicated global numbers, two different approaches were used. The first approach, called the difference in a limited approximation, is predicated on modifications in the overall electronic energy that occur when one electron is added or removed from

the neutral molecule. The basis of Koopman's hypothesis [35] is the difference in HOMO and LUMO energies for molecules. Equations five and six provide the Koopmans theory.

$$\chi = \frac{(E_{HOMO} + E_{LUMO})}{2} \dots\dots\dots 5$$

$$\eta = \frac{(E_{HOMO} - E_{LUMO})}{2} \dots\dots\dots 6$$

Electron states known as High Occupied Molecular Orbital (HOMO) and Low Unoccupied Molecular Orbital (LUMO) energies delineate particular sites where the orbitals of atoms and molecule mix linearly to generate energy-quantized electrons. The connection between the band gap in energy ( $E_g$ ) in Equations 7 and the difference in LUMO and HOMO [36] in Equation 6 is essential because it allows for predicting a material's properties based on its semiconductor, insulator, or conductor. A vital property of solids is the  $E_g$  property. It shows the energy differential between the level of complete energy and the virtual energy's lesser level [37]. Examine Figures 16 and 17. Table 6.

$$E_g = E_{LUMO} - E_{HOMO} \dots\dots\dots 7$$

#### The qualities of Electronegativity and Electrophilicity.

The ability of a molecule to absorb electrons is known as chemical electrophilicity, and it is based depends on the hardness and potential of chemicals, with hardness being defined as the ability to withstand to change and deformation. On the other hand, an atom's electronegativity is its ability to attract an electron density, which is An electron pair that is shared. Eqs. 8 and 9 provide the relationships needed to determine electronegativity and electrophilicity. [38]; see Table 7.

$$\chi = \frac{(E_{HOMO} + E_{LUMO})}{2} \dots\dots\dots 8$$

$$\omega = \frac{\chi^2}{2\eta} \dots\dots\dots 9$$

#### Electron of affinity and ionization potential.

The strength of the bond is determined by an atom's potential for ionization with an electron. Its energy is equal to the energy needed to extract a single electron from an A gas-phase atom. The energy released when an atom absorbs up electron is called "electron affinity." When one electron is taken out of a negatively charged ion, this energy is required. Eqs. 10 and 11 in Table 8 show that this is consistent with Koopman's hypothesis [39].

$$I.P = -E_{HOMO} \dots\dots\dots 10$$

$$E.A = -E_{LUMO} \dots\dots\dots 11$$

#### Acid Base (HSAB), Hardness, Softness Principles

In chemistry this idea explains the behavior of atoms or molecules as bases and acids. First, it needs to be demonstrated that hard and soft acids are acceptors, while Donors include both soft and hard grounds. Equations 12 and 13 that used to illustrate hardness, and softness, [40]

$$\eta = \frac{(IP - EA)}{2} \dots\dots\dots 12$$

$$\delta = \frac{1}{2\eta} \dots\dots\dots 13$$

The softness and hardness of chemicals are denoted the letters ( $\sigma$ ) and ( $\eta$ ), respectively. based on Table8. The following are the results of applying the same computational analyses to 4-(11-methyltriphenylen-2-yl)-1,2,3-selenadiazole with quinone's derivatives: In this study, a comparison of the HOMO energies for new compounds of charge-transfer complex is shown in Table 6 and it is found that the HOMO energy of MTSDQ1 compound is greater than that of MTSDQ2, MTSDQ3, and MTSDQ4 compounds. This is because MTSDQ1 is stronger and more stable, as a general rule of thumb states that the larger the HOMO-LUMO gap, the more stable the compound. The MTSDQ2 compound had the lowest HOMO energy in addition to the HOMO, which represents electron donors. The energy average, [41] in LUMO energy is arranged as

follows: From MTSDQ3 to MTSDQ1 to MTSDQ4 to MTSDQ2. Consequently, the MTSDQ1 molecule has the largest energy gap, whereas the MTSDQ4 compound has the smallest [42]. The energy in LUMO is as follows: MTSDQ3 > of other. can therefore aid in forecasting the location of pi ligand addition.

**Table 6.** The new group of charge-transfer compounds' electronic state.

Compound.	HOMO,(eV).	LUMO,(eV).	Eg,(eV).
MTSDQ1	-3.7185186	-2.46441	1.2541
MTSDQ2	-2.3977452	-1.6345	0.7632
MTSDQ3	-3.5612448	-2.65134	0.9099
MTSDQ4	-2.4630492	-1.75096	0.7121

In Table 7, the electronegativity of MTSDQ3 was greater than that of the other compounds, indicating that MTSDQ3 is the most reactive and MTSDQ2 is the least reactive. The electronegativity ( $\chi$ ) is a measure of an atom's attraction to electrons in a covalent bond, so compound MTSDQ3 does exhibit high charge flow. The results obtained also indicate that compound MTSDQ3 is strongly electrophilic, whereas compound MTSDQ2 is nucleophilic. The MTSDQ3 compound had the highest electrophilicity, while MTSDQ2 has the lowest electrophilicity among all prepared compounds for the same reason [43].

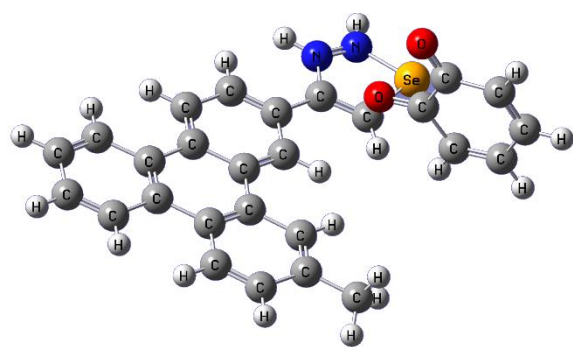
**Table 7.** Electrophilicity and electronegativity for novel group of charge-transfer complex synthesis.

Compound.	Electronegativity(eV) (X).	Electrophilicity (eV), (w).
MTSDQ1	3.091	7.621
MTSDQ2	2.016	5.326
MTSDQ3	3.106	10.6
MTSDQ4	2.107	6.234

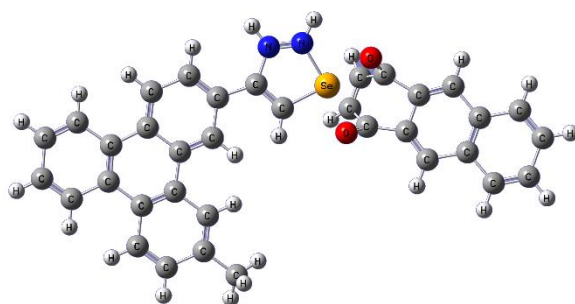
**Table 8.** Softness, hardness, electron affinity, and ionization potential for novel charge-transfer complex synthesis.

Compound	Ionization potential (eV) (I.P)	Electron affinity (eV) (E.A)	Softness ( $\delta$ )	Hardness ( $\eta$ )
MTSDQ1	3.7185	2.4644	1.595	0.627
MTSDQ2	2.3977	1.6345	2.62	0.382
MTSDQ3	3.5612	2.6513	2.198	0.455
MTSDQ4	2.463	1.751	2.809	0.356

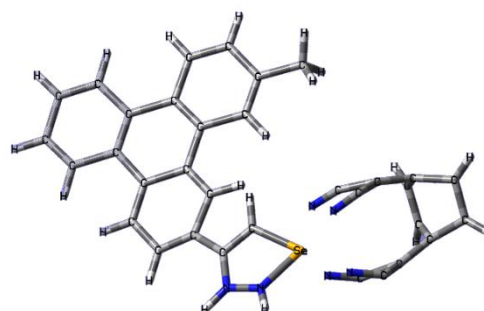
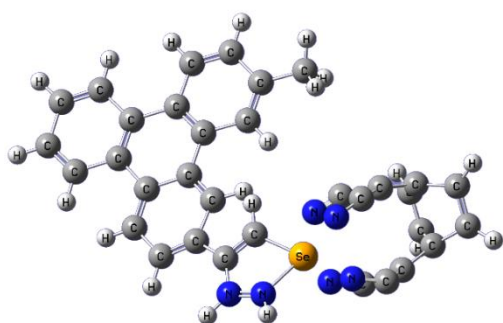
Table 8 shows that by comparing MTSDQ1, MTSDQ2, MTSDQ3, and MTSDQ4, the behavior of charge-transfer complex compounds can be categorized as donors or acceptors. Since MTSDQ1's hardness is higher than that of MTSDQ2, MTSDQ3, and MTSDQ4, it will act as a hard base. MTSDQ4 will act as a soft basis because its softness was higher than that of MTSDQ1, MTSDQ2, and MTSDQ3 [44].



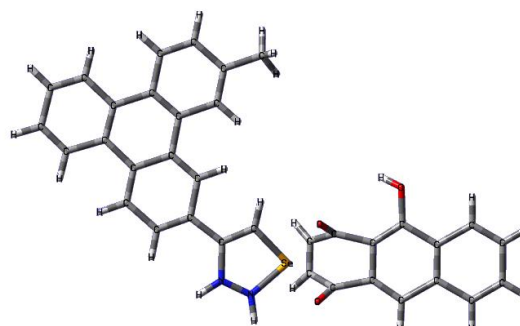
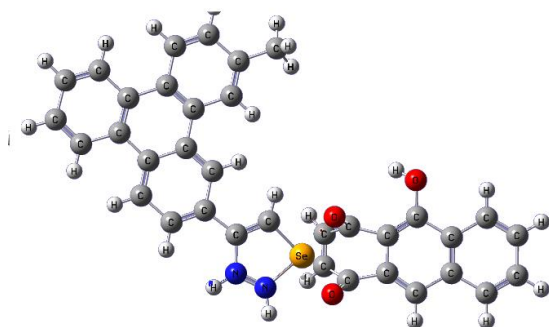
Compound (MTSDQ1).



Compound (MTSDQ2).

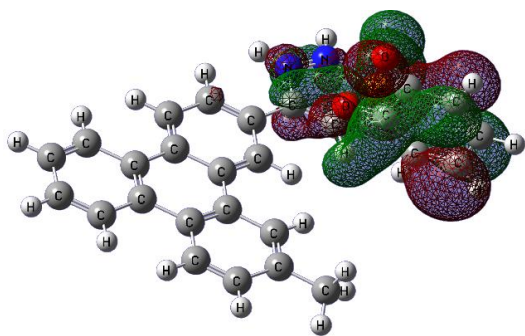


Compound (MTSDQ3).

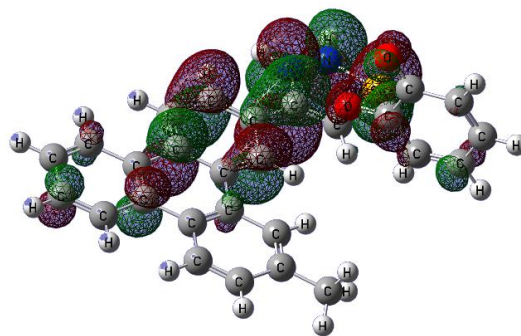


Compound (MTSDQ4).

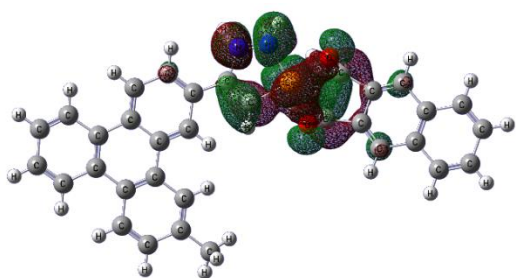
**Figure 16.** The structure of molecules tube and Ball model of charge-transfer complexes derivative of compound MTSD.



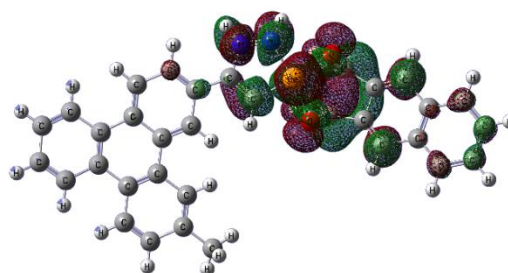
M.O (HOMO) of com. (MTSDQ1).



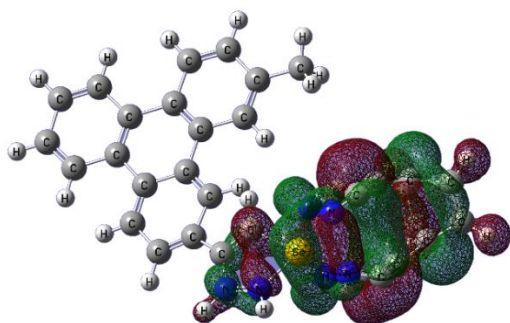
M.O (LUMO) of com. (MTSDQ1).



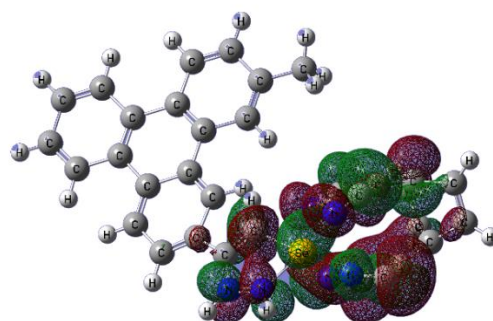
M.O (HOMO) of com. (MTSDQ2).



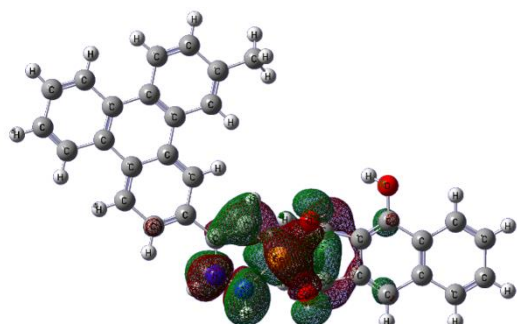
M.O (LUMO) of com. (MTSDQ2).



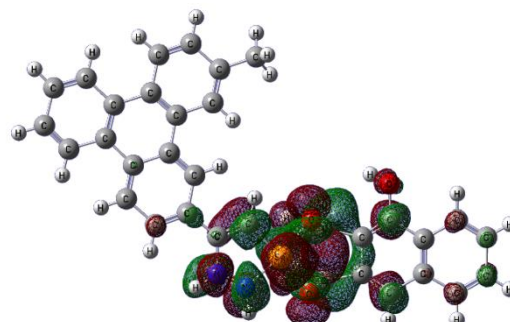
M.O (HOMO) of comp. (MTSDQ3).



M.O (LUMO) of com. (MTSDQ3).



M.O (HOMO) of com. (MTSDQ4).



M.O (LUMO) of com. (MTSDQ4).

Figure 17. Charge-transfer complexes molecular orbital HOMO and LUMO derivative of compound MTSD.

#### 4. Conclusion

This research succeeds in creating new charge-transfer complexes composed of 4-(11-methyltriphenylen-2-yl)-1,2,3-selenadiazole and different quinones which display notable electronic properties and molecular stability. The synthesized compounds exhibited different HOMO-LUMO energy gaps based on density functional theory (DFT) computational analysis which represented how efficiently the compounds transfer charges and react in their molecular structures. MTSDQ1 possessed the most considerable energy gap that indicated better molecular stability yet MTSDQ4 demonstrated lesser energy gap and hence exhibited stronger reactivity properties. These research findings present possible usages of charge-transfer complexes in next-generation electronic devices including organic semiconductors alongside photodetectors. Future research should focus on device fabrication methods that incorporate these complexes while broadening derivative quinone investigations regarding their effect on electronic device performance.

#### REFERENCES

- [1] Z. Chen, Y. Li, Z. He, Y. Xu, and W. Yu, "Theoretical investigations on charge transport properties of tetrabenzo [a, d, j, m] coronene derivatives using different density functional theory functionals (B3LYP, M06-2X, and wB97XD)," *J. Chem. Res.*, vol. 43, no. 7-8, pp. 293-303, 2019.
- [2] F. Juliá, "Ligand-to-metal charge transfer (LMCT) photochemistry at 3d-metal complexes: an emerging tool for sustainable organic synthesis," *ChemCatChem*, vol. 14, no. 19, p. e202200916, 2022.
- [3] X. Chen, X. Zhang, X. Xiao, Z. Wang, and J. Zhao, "Recent Developments on Understanding Charge Transfer in Molecular Electron Donor-Acceptor Systems," *Angew. Chem. Int. Ed.*, vol. 62, no. 16, p. e202216010, 2023.
- [4] S. Jung, Y. Cho, S. H. Kang, S. J. Yoon, and C. Yang, "Effect of third component on efficiency and stability in ternary organic solar cells: more than a simple superposition," *Sol. RRL*, vol. 6, no. 2, p. 2100819, 2022.
- [5] H. Anabestani, S. Nabavi, and S. Bhadra, "Advances in flexible organic photodetectors: Materials and applications," *Nanomaterials*, vol. 12, no. 21, p. 3775, 2022.
- [6] F. Tohidi, S. G. Holagh, and A. Chitsaz, "Thermoelectric Generators: A comprehensive review of characteristics and applications," *Appl. Therm. Eng.*, vol. 201, p. 117793, 2022.
- [7] Q. Zhang, K. Deng, L. Wilkens, H. Reith, and K. Nielsch, "Micro-thermoelectric devices," *Nat. Electron.*, vol. 5, no. 6, pp. 333-347, 2022.
- [8] A. Mukherjee et al., "Vertical architecture solution-processed quantum dot photodetectors with amorphous selenium hole transport layer," *ACS Photonics*, vol. 10, no. 1, pp. 134-146, 2022.
- [9] V. Selamneni, V. Adepur, H. Raghavan, and P. Sahatiya, "Ultra-high responsivity and enhanced trap assisted charge transfer by utilizing Ti3C2TX (MXene) as a transport layer for ReS2 based flexible broadband photodetector: a better alternative to graphene," *FlatChem*, vol. 33, p. 100363, 2022.
- [10] T. I. Alanazi and A. M. El Sayed, "Structural, optical analysis, stress-strain, and dielectric properties of selenium oxide/LaFeO3/blend nanocomposites with tunable properties for optoelectronics and micro-supercapacitors," *J. Energy Storage*, vol. 95, p. 112652, 2024.
- [11] W. Ma et al., "Synergetic contribution of enriched selenium vacancies and out-of-plane ferroelectric polarization in AB-stacked MoSe2 nanosheets as efficient piezocatalysts for TC degradation," *New J. Chem.*, vol. 46, no. 10, pp. 4666-4676, 2022.
- [12] K. Kang et al., "Switchable moiré potentials in ferroelectric WTe2/WSe2 superlattices," *Nat. Nanotechnol.*, vol. 18, no. 8, pp. 861-866, 2023.
- [13] A. Majumdar et al., "A critical review on the organo-metal (loid) s pollution in the environment: Distribution, remediation and risk assessment," *Sci. Total Environ.*, p. 175531, 2024.
- [14] R. Ali and R. Siddiqui, "Dithieno [3, 2-b: 2', 3'-d] thiophene (DTT): An emerging heterocyclic building block for future organic electronic materials & functional supramolecular chemistry," *RSC Adv.*, vol. 12, no. 55, pp. 36073-36102, 2022.
- [15] A. Madabeni, *A Theoretical Mechanistic Journey into Organoselenium (Bio) Chemistry: from Elementary Molecular Models to Catalysis*, 2024.
- [16] A. Arora et al., "Molecular organosulphur, organoselenium and organotellurium complexes as homogeneous transition metal catalytic systems for Suzuki coupling," *ChemistrySelect*, vol. 7, no. 33, p. e202201704, 2022.

- [17] A. Madabeni et al., "50 Years of Organoselenium Chemistry, Biochemistry and Reactivity: Mechanistic Understanding, Successful and Controversial Stories," *Chem.–Eur. J.*, vol. 30, no. 70, p. e202403003, 2024.
- [18] F. Marini, L. Bagnoli, and M. Palomba, "Synthesis of organochalcogens: use of nonconventional solvents/reaction media," in *Organochalcogen Compounds*, Elsevier, 2022, pp. 147-192.
- [19] A. J. Pacuła-Miszewska and L. Sancineto, "Oxygen-transfer reactions catalyzed by organoselenium compounds," in *Organochalcogen Compounds*, Elsevier, 2022, pp. 219-250.
- [20] M. S. More, P. G. Joshi, Y. K. Mishra, and P. K. Khanna, "Metal complexes driven from Schiff bases and semicarbazones for biomedical and allied applications: a review," *Mater. Today Chem.*, vol. 14, p. 100195, 2019.
- [21] A. A. Jadhav, P. V. More, and P. K. Khanna, "Rapid microwave synthesis of white light emitting magic sized nano clusters of CdSe: role of oleic acid," *RSC Adv.*, vol. 5, no. 94, pp. 76733-76742, 2015.
- [22] Y. Zhou and H. Heimgartner, "Selenium-Containing Heterocycles from Isoselenocyanates: Synthesis of 1,2,3-Selenadiazole Derivatives," *Helv. Chim. Acta*, vol. 83, no. 3, pp. 539-553, 2000.
- [23] O. V. Stepanova et al., "Synthesis of 4-(2-Fluoro-4-hydroxyphenyl)-1,2,3-thia-and-Selenadiazoles and Glycosides on Their Base," *Russ. J. Gen. Chem.*, vol. 90, pp. 1241-1248, 2020.
- [24] H. S. Mohammed and N. H. Al-Saadawy, "Synthesis, characterization and theoretical investigation of innovative charge-transfer complexes derived from the N-phenyl 3,4-selenadiazobenzophenone imine," *Baghdad Sci. J.*, vol. 20, no. 5 (Suppl.), 2023.
- [25] H. S. Mohammed and N. H. Al-Saadawy, "Synthesis, characterization, and theoretical study of novel charge-transfer complexes derived from 3,4-selenadiazobenzophenone," *Indones. J. Chem.*, vol. 22, no. 6, pp. 1663-1672, 2022.
- [26] R. M. Silverstein and G. C. Bassler, "Spectrometric identification of organic compounds," *J. Chem. Educ.*, vol. 39, no. 11, p. 546, 1962.
- [27] G. Du, K. Y. Wang, J. Ran, F. Y. Wang, and Z. X. Pan, "Application of IR/SEM and other modern instruments for mineral identification," *Rock Miner. Anal.*, vol. 33, no. 5, pp. 625-633, 2014.
- [28] M. Krupová, J. Kessler, and P. Bouř, "Recent trends in chiroptical spectroscopy: theory and applications of vibrational circular dichroism and Raman optical activity," *ChemPlusChem*, vol. 85, no. 3, pp. 561-575, 2020.
- [29] Z. Moussa et al., "First exclusive stereo- and regioselective preparation of 5-arylimino-1,3,4-selenadiazole derivatives: Synthesis, NMR analysis, and computational studies," *Chem.–Asian J.*, vol. 18, no. 17, p. e202300475, 2023.
- [30] V. A. Potapov et al., "Stereoselective synthesis of E-2-halovinyl tellanes, ditellanes and selenides based on tellurium tetrahalides, selenium dihalides and internal alkynes," *J. Organomet. Chem.*, vol. 867, pp. 300-305, 2018.
- [31] M. Malček et al., "Formation of metal-radical species upon reduction of late transition metal complexes with heteroleptic ligands: An experimental and theoretical study," *New J. Chem.*, vol. 44, no. 30, pp. 13195-13206, 2020.
- [32] Y. Ishigaki et al., "Molecular recognition by chalcogen bond: selective charge-transfer crystal formation of dimethylnaphthalene with selenadiazolotetracyanonaphthoquinodimethane," *Eur. J. Org. Chem.*, vol. 2021, no. 6, pp. 990-997, 2021.
- [33] A. H. Raheem, K. J. Al-Shejry, and E. D. Al-Bermany, "Density functional theory calculations for methylbenzene molecules group," *Br. J. Sci.*, vol. 5, pp. 57-64, 2012.
- [34] X. Wang and T. C. Berkelbach, "Excitons in solids from periodic equation-of-motion coupled-cluster theory," *J. Chem. Theory Comput.*, vol. 16, no. 5, pp. 3095-3103, 2020.
- [35] A. M. Khuodhair, F. N. Ajeel, and M. O. Oleiwi, "Density functional theory investigations for the electronic and vibrational properties of donor-acceptor system," *J. Appl. Phys. Sci. Int.*, vol. 6, no. 4, pp. 202-209, 2016.
- [36] R. M. Kubba, M. A. Mohammed, and L. S. Ahamed, "DFT calculations and experimental study to inhibit carbon steel corrosion in saline solution by quinoline-2-one derivative: Carbon steel corrosion," *Baghdad Sci. J.*, vol. 18, no. 1, p. 0113, 2021.
- [37] A. S. Alwan, S. K. Ajeel, and M. L. Jabbar, "Theoretical study for Coronene and Coronene-Al, B, C, Ga, In and Coronene-O interactions by using density functional theory," *Univ. Thi-Qar J.*, vol. 14, no. 4, pp. 1-14, 2019.
- [38] H. M. Abd El-Lateef et al., "Synthesis, experimental, and computational studies of water soluble anthranilic organoselenium compounds as safe corrosion inhibitors for J55 pipeline steel in acidic oilfield formation water," *Colloids Surf. A Physicochem. Eng. Asp.*, vol. 625, p. 126894, 2021.

- [39] M. L. Jabbar, "Theoretical study for the interactions of Coronene-Y interactions by using Density functional theory with hybrid function," *Univ. Thi-Qar J.*, vol. 13, no. 3, pp. 28–41, 2018.
- [40] V. Coropceanu *et al.*, "Vibronic coupling in organic semiconductors: the case of fused polycyclic benzene–thiophene structures," *Chem.–Eur. J.*, vol. 12, no. 7, pp. 2073–2080, 2006.
- [41] A. J. Hameed, M. Ibrahim, and H. ElHaes, "Computational notes on structural, electronic and QSAR properties of [C60] fulleropyrrolidine-1-carbodithioic acid 2; 3 and 4-substituted-benzyl esters," *J. Mol. Struct. THEOCHEM*, vol. 809, no. 1–3, pp. 131–136, 2007.
- [42] H. G. Kim and H. J. Choi, "Thickness dependence of work function, ionization energy, and electron affinity of Mo and W dichalcogenides from DFT and GW calculations," *Phys. Rev. B*, vol. 103, no. 8, p. 085404, 2021.
- [43] M. L. Jabbar and K. J. Kadhim, "Electronic properties of doped graphene nanoribbon and the electron distribution contours: A DFT study," *Russ. J. Phys. Chem. B*, vol. 15, pp. 46–52, 2021.
- [44] M. J. Sani, "Spin-orbit coupling effect on the electrophilicity index, chemical potential, hardness and softness of neutral gold clusters: A relativistic ab-initio study," *HighTech Innov. J.*, vol. 2, no. 1, pp. 38–50, 2021.